NASA Technical Memorandum 1-06177
ICOMP–93–20; CMOTT–93–08

A Vorticity Dynamics Based Model for the Turbulent Dissipation—Model Development and Validation

Tsan-Hsing Shih, William W. Liou, Aamir Shabbir, Zhigang Yang, and Jian Zhu
Institute for Computational Mechanics in Propulsion
and Center for Modeling of Turbulence and Transition
Lewis Research Center
Cleveland, Ohio

January 1994

NASA

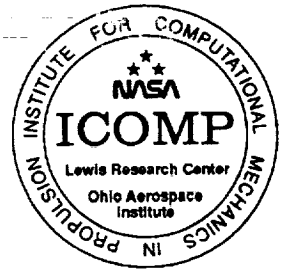

A Vorticity Dynamics Based Model for the Turbulent Dissipation—Model Development and Validation

Tsan-Hsing Shih, William W. Liou, Aamir Shabbir,
Zhigang Yang, and Jiang Zhu
Institute for Computational Mechanics in Propulsion
and Center for Modeling of Turbulence and Transition
Lewis Research Center
Cleveland, Ohio 44135

Abstract

A new model dissipation rate equation is proposed based on the dynamic equation of the mean-square vorticity fluctuation for large Reynolds number turbulence. The advantage of working with the vorticity fluctuation equation is that the physical meanings of the terms in this equation are more clear than those in the dissipation rate equation. Hence, the model development based on the vorticity fluctuation equation is more straightforward. The resulting form of the model equation is consistent with the spectral energy cascade analysis introduced by Lumley (1992). The proposed model dissipation rate equation is numerically well behaved and can be applied in conjunction with any level of turbulence closure. In the present study, it is applied to a realizable eddy viscosity model. Flows that are examined include: (i) rotating homogeneous shear flows; (ii) free shear flows; (iii) a channel flow and flat plate boundary layers with and without pressure gradients; and (iv) backward facing step separated flows. In most cases, the present model predictions show considerable improvement over the standard $k-\varepsilon$ model.

1. Introduction

The dissipation rate equation is often used in various turbulence closure schemes. Its exact equation can be written as,

$$\begin{aligned}\varepsilon_{,t} + U_i\varepsilon_{,i} =& \nu\varepsilon_{,ii} - (\overline{\varepsilon' u_i})_{,i} - \frac{2\nu}{\rho}(\overline{p_{,k}u_{i,k}})_{,i} \\ & - 2\nu\overline{u_j u_{i,k}}U_{i,kj} - 2\nu\overline{u_{i,k}u_{j,k}}U_{i,j} \\ & - 2\nu\overline{u_{i,j}u_{i,k}}U_{j,k} - 2\nu\overline{u_{i,k}u_{j,k}u_{i,j}} \\ & - 2\nu^2\overline{u_{i,jk}u_{i,jk}}\end{aligned} \tag{1}$$

where $\varepsilon = \nu\overline{u_{i,j}u_{i,j}}$ and $\varepsilon' = \nu u_{i,j}u_{i,j}$. All the terms on the right hand side of Eq. (1), except the viscous diffusion term $\nu\varepsilon_{,ii}$, are new unknowns. Thus, they must be modeled before this equation can be used for applications. Modeling of these new unknowns, which are related the small scales of turbulence, is extremely difficult due to the lack of a clear understanding of their physical meanings. Therefore, in the literature, Eq. (1) has not been considered as a useful equation to work with. One often ignores Eq. (1) and creates a model dissipation rate equation which has a structure similar to that of the turbulent kinetic energy equation. In other words, the dissipation rate equation also has generation and destruction terms which are assumed to be proportional to the production and dissipation terms in the turbulent kinetic energy equation over the period of large eddy turn-over time, k/ε. With this assumption, the resulting model dissipation rate equation can be written in the following form:

$$\begin{aligned}\varepsilon_{,t} + U_i\varepsilon_{,i} =& \nu\varepsilon_{,ii} - (\overline{\varepsilon' u_i})_{,i} \\ & - C_{\varepsilon 1}\frac{\varepsilon}{k}\overline{u_i u_j}U_{i,j} - C_{\varepsilon 2}\frac{\varepsilon^2}{k}\end{aligned} \tag{2}$$

Eq.(2) is the standard model dissipation rate equation which has been widely used in various turbulence closure schemes. In addition, several modified versions of Eq.(2) have also been also proposed for different applications, for example, in near-wall turbulent flows[1-4] and in rotating turbulent flows[5].

Recently, Lumley[6] proposed a dissipation rate equation based on the concept of non-equilibrium spectral energy transfer due to the interactions between eddies of different sizes. A new transport equation for an inverse time scale has also been suggested in conjunction with his new ε equation which is of a different form from that of Eq.(2). This

model mimics the physics of the statistical energy transfer from large eddies to small eddies and is successful in the prediction of various turbulent free shear flows[6].

In this paper, we explore the possibility of deriving a new model form for the dissipation equation which is not only more physically related to the original ε equation but also simpler and more robust than the standard dissipation equation (2). This is achieved by first developing a model equation for the the dynamic equation for the mean-square vorticity fluctuation $\overline{\omega_i\omega_i}$. Once the dynamic equation for $\overline{\omega_i\omega_i}$ is modeled, a model dissipation rate equation can be readily obtained.

2. Dynamic equation for $\overline{\omega_i\omega_i}$

The exact equation for $\overline{\omega_i\omega_i}$ is

$$\begin{aligned}(\frac{\overline{\omega_i\omega_i}}{2})_{,t} + U_j(\frac{\overline{\omega_i\omega_i}}{2})_{,j} = \nu(\frac{\overline{\omega_i\omega_i}}{2})_{,jj} - \frac{1}{2}(\overline{u_j\omega_i\omega_i})_{,j} \\ + \overline{\omega_i u_{i,j}}\Omega_j - \overline{u_j\omega_i}\Omega_{i,j} \\ + \overline{\omega_i\omega_j}U_{i,j} + \overline{\omega_i\omega_j u_{i,j}} \\ - \nu\overline{\omega_{i,j}\omega_{i,j}}\end{aligned} \tag{3}$$

where u_i and U_i are the fluctuating and mean velocities, and ω_i and Ω_i are the fluctuating and mean vorticities which are defined by

$$\omega_i = \epsilon_{ijk}u_{k,j}, \qquad \Omega_i = \epsilon_{ijk}U_{k,j} \tag{4}$$

Tennekes and Lumley[7] clearly described the physical meaning of each term in Eq.(3). The first two terms on the right hand side represent the viscous transport and the turbulent transport of $\overline{\omega_i\omega_i}$, respectively . The third term is the source term which is produced by fluctuating vortex stretching and mean vorticity. This term also appears in the equation for $\Omega_i\Omega_i$ with the same sign, hence, it will either increase or decrease $\Omega_i\Omega_i$ and $\overline{\omega_i\omega_i}$ simultaneously. The fourth term represents the vorticity exchange between $\overline{\omega_i\omega_i}$ and $\Omega_i\Omega_i$, because it appears with opposite sign in the equation for $\Omega_i\Omega_i$. The fifth term represents the source produced by mean vortex stretching. The sixth and seventh terms are the production due to fluctuating vortex stretching and the dissipation due to the viscosity of the fluid, respectively. Tennekes and Lumley[7] have shown that, at sufficiently high turbulent Reynolds numbers, the sixth and the seventh terms are the largest terms in

Eq.(3). That is,

$$\overline{\omega_i\omega_j u_{i,j}}, \nu\overline{\omega_{i,j}\omega_{i,j}} \approx \mathcal{O}(\frac{u^3}{l^3}R_t^{3/2})$$

The first, the third, the forth, and the fifth terms are the smallest, either of order (u^3/l^3) or $(u/l)^3 R_t^{\frac{1}{2}}$. In the above analysis, "$\mathcal{O}$" denotes the order of magnitude. $R_t = ul/\nu$ is the turbulent Reynolds number. u and l are the characteristic velocity and length scales of turbulence, respectively. If the terms of order $(u^3/l^3)R_t$ or larger were kept in equation (3), then the evolution of $\overline{\omega_i\omega_i}$ should be described by the following equation,

$$(\frac{\overline{\omega_i\omega_i}}{2})_{,t} + U_j(\frac{\overline{\omega_i\omega_i}}{2})_{,j} = -\frac{1}{2}(\overline{u_j\omega_i\omega_i})_{,j} + \overline{\omega_i\omega_j u_{i,j}} - \nu\overline{\omega_{i,j}\omega_{i,j}} \tag{5}$$

As pointed out by Tennekes and Lumley[7], at large Reynolds numbers, Eq.(5) becomes,

$$\overline{\omega_i\omega_j u_{i,j}} = \nu\overline{\omega_{i,j}\omega_{i,j}} \tag{6}$$

Or equivalently, production equals dissipation. This relation indicates that the term $\overline{\omega_i\omega_j u_{i,j}}$ is always positive. In addition, it indicates that there is a new length scale created by the vortex stretching which is related to the derivative of fluctuating vorticities. The vortex stretching tends to reduce the size of eddies and to create a broad spectrum of eddy sizes. However, this process must end at a certain level of eddy size because of the smoothing effect of viscosity. We expect that the terminal eddy size is the Kolmogorov microscale which corresponds to the length scale of the derivative of fluctuating vorticity $\omega_{i,j}$. This can be easily verified from Eq.(6).

In the following, a model equation for the mean-square vorticity fluctuation will first be developed. The proposed model dissipation is then derived straightforwardly.

3. Modeling of the dynamic equation for $\overline{\omega_i\omega_i}$

3.1 Modeling of $\overline{\omega_i\omega_j u_{i,j}}$

We first define a fluctuating anisotropic tensor b_{ij}^{ω} using $\omega_i\omega_j$

$$b_{ij}^{\omega} = \frac{\omega_i\omega_j}{\omega_k\omega_k} - \frac{1}{3}\delta_{ij} \tag{7}$$

then

$$\overline{\omega_i\omega_j u_{i,j}} = \overline{b_{ij}^{\omega}\omega_k\omega_k u_{i,j}} \tag{8}$$

We expect that the vortex stretching tends to align vortex lines with the strain rate and that the anisotropy b_{ij}^{ω} is mainly due to the fluctuating strain rate; hence, the anisotropy b_{ij}^{ω} may be assumed to be proportional to the strain rate s_{ij}. That is,

$$b_{ij}^{\omega} \propto \frac{s_{ij}}{s}, \tag{9}$$

where

$$s = (2s_{ij}s_{ij})^{1/2}, \quad s_{ij} = (u_{i,j} + u_{j,i})/2$$

This leads to

$$\overline{\omega_i\omega_j u_{i,j}} \propto \overline{\omega_k\omega_k \frac{s_{ij}u_{i,j}}{s}} = \overline{\omega_k\omega_k\ s} \tag{10}$$

If we further assume that $\omega_k\omega_k$ and $(2s_{ij}s_{ij})^{1/2}$ are well correlated, we may write

$$\overline{\omega_i\omega_j u_{i,j}} \propto \overline{\omega_k\omega_k}\ \sqrt{\overline{2s_{ij}s_{ij}}} \tag{11}$$

Noting that $\overline{\omega_i\omega_i} = 2\overline{s_{ij}s_{ij}}$ at large Reynolds numbers, we may also write

$$\overline{\omega_i\omega_j u_{i,j}} \propto \overline{\omega_k\omega_k}\ \sqrt{\overline{\omega_i\omega_i}} = \frac{\overline{\omega_k\omega_k}\ \overline{\omega_i\omega_i}}{\sqrt{\overline{\omega_i\omega_i}}} \tag{12}$$

Eqs.(11) and (12) indicate that the model for $\overline{\omega_i\omega_j u_{i,j}}$ is of order $(u^3/\ell^3)R_t^{3/2}$ as it should be.

3.2 Modeling of $\overline{\omega_i\omega_j u_{i,j}} - \nu\overline{\omega_{i,j}\omega_{i,j}}$

Eq.(2) indicates that $\overline{\omega_i\omega_j u_{i,j}} - \nu\overline{\omega_{i,j}\omega_{i,j}}$ must be of order $(u^3/\ell^3)R_t$. Therefore, $-\nu\overline{\omega_{i,j}\omega_{i,j}}$ must cancel $\overline{\omega_k\omega_k}\ \overline{\omega_i\omega_i}/\sqrt{\overline{\omega_i\omega_i}}$ (or $\overline{\omega_k\omega_k}\ \sqrt{\overline{2s_{ij}s_{ij}}}$) in such a way that their difference is smaller than $\overline{\omega_k\omega_k}\ \overline{\omega_i\omega_i}/\sqrt{\overline{\omega_i\omega_i}}$ (or $\overline{\omega_k\omega_k}\ \sqrt{\overline{2s_{ij}s_{ij}}}$) by an order of $R_t^{1/2}$. This suggests that the sum of these two terms can be related to the following two terms:

$$\overline{\omega_k\omega_k}\ S, \qquad \frac{\overline{\omega_k\omega_k}\ \overline{\omega_i\omega_i}}{\frac{k}{\nu} + \sqrt{\overline{\omega_i\omega_i}}} \tag{13}$$

since both the ratio of k/ν to $\sqrt{\overline{\omega_i\omega_i}}$ and the ratio of s to S are of order $R_t^{1/2}$. $k(\approx u^2)$ denotes the turbulent kinetic energy and S is the mean strain rate $(\sqrt{2S_{ij}S_{ij}})$. As a result, the dynamic equation for fluctuating vorticity can be modeled as

$$\begin{aligned}(\frac{\overline{\omega_i\omega_i}}{2})_{,t} + U_j(\frac{\overline{\omega_i\omega_i}}{2})_{,j} = -\frac{1}{2}(\overline{u_j\omega_i\omega_i})_{,j} + C_1\overline{\omega_k\omega_k}S \\ - C_2\frac{\overline{\omega_k\omega_k}\ \overline{\omega_i\omega_i}}{\frac{k}{\nu} + \sqrt{\overline{\omega_i\omega_i}}}\end{aligned} \tag{14}$$

Here, the term $\overline{\omega_k\omega_k}S$ represents the part of the production term $\overline{\omega_i\omega_j u_{i,j}}$ due to the mean strain rate which is always positive if $S \neq 0$. Note that the sum of last two terms in Eq.(14) models the last two terms in Eq.(6) as a whole and should not be viewed as a model for either individual term.

4. Modeling of the dissipation rate equation

Noting that at large Reynolds number $\overline{\omega_i\omega_i} = \overline{u_{i,j}u_{i,j}}$ and $\varepsilon = \nu\overline{\omega_i\omega_i}$, we readily obtain a modeled dissipation rate equation,

$$\varepsilon_{,t} + U_j\ \varepsilon_{,j} = -(\overline{u_j\varepsilon'})_{,j} + C_1 S\ \varepsilon - C_2\frac{\varepsilon^2}{k+\sqrt{\nu\varepsilon}} \tag{15}$$

where the model coefficients, C_1 and C_2, are expected to be independent of the Reynolds number as the Reynolds number becomes large. We note that C_1 and C_2 may be affected by the solid body rotation imposed on turbulence through the reduction of fluctuation vortex stretching, $\overline{\omega_i\omega_j u_{i,j}}$, as was shown by Bardina[5]; however, this effect is rather weak compared to the other mechanisms. For example, Reynolds stresses will be first substantially affected by rotation and result in a substantial change of the turbulent field, say k, as shown in the calculation of the rotating homogeneous shear flows in section 5.1. This will also affect the evolution of ε through, say, k. The signs of C_1 and C_2 can be easily determined. For example, in a decaying grid turbulence, only the last term on the right hand side of Eq.(15) is non-zero and must be negative, hence C_2 must be positive. For the case of homogeneous shear flow, both the turbulent kinetic energy and its dissipation rate increase with time so that the source term in Eq.(15) must be positive hence C_1 must be positive. In fact, these two types of flows[8,9] will be used for calibrating the values of C_1 and C_2.

The differences between the present model dissipation rate equation, Eq.(15), and the standard model dissipation rate equation, Eq.(2), are the following. First, the "destruction" term is well behaved so that Eq.(15) does not have a singularity anywhere in the flow field. This is due to the presence of $\sqrt{\nu\varepsilon}$. Although $\sqrt{\nu\varepsilon}$ is a term of lower order than that of k at large Reynolds numbers, it is kept here to avoid the singularity in case $k \to 0$. Second, the Reynolds stresses do not appear in Eq.(15). Consequently, the present model dissipation rate equation will be more robust than the standard model dissipation rate equation when it is used in conjunction with second-order closure schemes, since S

normally behaves better than the Reynolds stresses in numerical calculations, especially for cases with poor initial conditions. In addition, the present form of the "production" term is similar to that proposed by Lumley[2] which is based on the concept of spectral energy transfer. It is believed that the present model describes the turbulent vortex stretching and dissipation terms more appropriately.

Eq.(15) can be applied in conjunction with any level of turbulence closures. However, the turbulent transport term $(\overline{\varepsilon' u_i})_{,i}$ needs to be modeled differently at different levels of turbulence modeling. Here, we apply Eq.(15) to a realizable eddy viscosity model of Shih *et al.*[10], and $(\overline{\varepsilon' u_i})_{,i}$ is modeled as

$$(\overline{\varepsilon' u_i})_{,i} = -(\frac{\nu_T}{\sigma_\varepsilon}\varepsilon_{,i})_{,i} \tag{16}$$

For completeness, the realizable eddy viscosity model will be briefly described in the following section. The model coefficients C_1, C_2 and σ_ε will be determined later.

4.1 A realizable eddy viscosity model

Shih *et al.*[10] proposed a realizable Reynolds stress algebraic equation model. Here, for simplicity, we adopt its linear form:

$$-\overline{u_i u_j} = \nu_T(U_{i,j} + U_{j,i}) - \frac{2}{3}k\delta_{ij} \tag{17}$$

$$\nu_T = C_\mu \frac{k^2}{\varepsilon}, \qquad C_\mu = \frac{2/3}{1.25 + \eta + 0.9\xi} \tag{18}$$

where,

$$\eta = \frac{kS}{\varepsilon}, \quad \xi = \frac{k\Omega}{\varepsilon}, \quad S = \sqrt{2S_{ij}S_{ij}}, \quad \Omega = \sqrt{2\Omega^*_{ij}\Omega^*_{ij}} \tag{19}$$

and

$$S_{ij} = \frac{1}{2}(U_{i,j} + U_{j,i}), \qquad \Omega^*_{ij} = \frac{1}{2}(U_{i,j} - U_{j,i}) + 4\epsilon_{rmji}\omega_{rm} \tag{20}$$

where ω_{rm} is the rotation rate of the coordinate frame.

The modeled k and ε equations are

$$k_{,t} + U_j k_{,j} = (\frac{\nu_T}{\sigma_k}k_{,j})_{,j} - \overline{u_i u_j}U_{i,j} - \varepsilon \tag{21}$$

$$\varepsilon_{,t} + U_j \varepsilon_{,j} = (\frac{\nu_T}{\sigma_\varepsilon}\varepsilon_{,j})_{,j} + C_1 S\,\varepsilon - C_2\frac{\varepsilon^2}{k + \sqrt{\nu\varepsilon}} \tag{22}$$

where C_1, C_2, σ_k and σ_ε are model constants.

4.2 Model constants C_1, C_2 and σ_ε

In decaying grid turbulence at large Reynolds number, the equations for turbulent kinetic energy k and its dissipation rate ε are

$$\begin{aligned} k_{,t} &= -\varepsilon \\ \varepsilon_{,t} &= -C_2 \frac{\varepsilon^2}{k} \end{aligned} \tag{23}$$

Let

$$\frac{k}{k_0} = (\frac{t}{t_0})^{-n}, \qquad \frac{\varepsilon}{\varepsilon_0} = (\frac{t}{t_0})^{-\alpha}$$

The following equations can be obtained from the k and ε equations:

$$\alpha = n+1, C_2 = \frac{n+1}{n} \tag{24}$$

Experiments[8] show that the decay exponent n varies from 1.08 to 1.30. In this study we choose $C_2 = 1.9$ which corresponds to $n = 1.11$. After C_2 is chosen, we use the experimental data for homogeneous shear flow[9] to calibrate the value of C_1 which is found to be about 0.42.

The value of σ_ε will be estimated by using the log-law in turbulent boundary layers. These relations are:

$$\begin{aligned} \frac{U}{u_\tau} &= \frac{1}{\kappa} \log \frac{u_\tau y}{\nu} + C \\ -\overline{uv} &\approx u_\tau^2, \qquad -\overline{uv}\frac{\partial U}{\partial y} \approx \varepsilon \end{aligned} \tag{25}$$

which lead to the following,

$$\begin{aligned} \frac{k}{u_\tau^2} &= \frac{1}{\sqrt{C_\mu}}, \quad \frac{\partial U}{\partial y} = \frac{u_\tau}{\kappa y}, \quad \varepsilon = \frac{u_\tau^3}{\kappa y} \\ \eta = \xi &= \frac{k}{\varepsilon}\frac{\partial U}{\partial y} = \frac{k}{u_\tau^2} = \frac{1}{\sqrt{C_\mu}} \end{aligned} \tag{26}$$

Substituting the η and ξ above into the Eq.(18) for C_μ, we obtain

$$1.25\ C_\mu + 1.9\ \sqrt{C_\mu} - \frac{2}{3} = 0 \tag{27}$$

which gives $C_\mu = 0.0864$ in the log-law region. This value is then used below to determine σ_ε.

Analyzing the dissipation rate equation in the log-law region, we obtain

$$\sigma_\varepsilon = \frac{\kappa^2}{C_2\sqrt{C_\mu} - C_1} = 1.21 \tag{28}$$

where the von Karman constant $\kappa = 0.41$. The model constants are summarized in the Table 1.

Table 1. Model constants

σ_k	σ_ε	C_1	C_2
1.0	1.21	0.42	1.9

5. Model applications

The results of some turbulent flow calculations using the proposed new turbulence model, Eqs.(17)-(22), are shown in this section. These include (i) rotating homogeneous shear flows, (ii) free shear flows, (iii) channel flow and boundary layers with and without pressure gradients, and (v) backward-facing step flows. The computations with the present and the standard $k-\varepsilon$ models are compared with DNS, LES and various experiments.

5.1 Rotating homogeneous shear flows

The comparisons are made with the large eddy simulation of Bardina *et al.*[5] for four different cases of Ω/S (which are Ω/S=0.0, Ω/S=-0.50, Ω/S=0.25, and Ω/S=0.50). The initial conditions in all these cases correspond to isotropic turbulence and $\epsilon_0/Sk_0 = 0.297$. Figure 1 (a) compares the evolution of turbulence kinetic energy, normalized by its initial value k_0, with the non-dimensionalized time St for $\Omega/S = 0.0$. For this case both the present and the standard $k-\epsilon$ (denoted by ske hereafter) models show the trends exhibited by LES, with the present model being closer to the LES data. Figure 1 (b) shows the comparisons for the case $\Omega/S = 0.25$. The ske model does not pick the effect of rotation on turbulence as it gives the same growth rate of turbulence kinetic energy as it did for the

no rotation case, a result which is already known. On the other hand the present model is in reasonable agreement with the LES data as it shows a faster growth of the turbulence kinetic energy with time over the no rotation case. Figures 1 (c) and 1 (d) compare the evolution of turbulence kinetic energy for two more cases of $\Omega/S = 0.5$ and $\Omega/S = -0.5$. For the first of these cases the LES shows that the growth rate of the turbulence kinetic energy is decreased over the no rotation rate case. The present model is able to pick up this trend and although the agreement between the present model and the LES is not as good as it is for the other cases, it still is a lot better than the ske model. For the case of $\Omega/S = -0.5$ the agreement between the present model and the LES is quite reasonable. It should be pointed out that the rotation effect on turbulence is brought about by the C_μ formulation of Eq. (18).

5.2 Free shear flows

Calculations using the present and the ske models were performed for a mixing layer, a plane jet and a round jet. Figures 2, 3 and 4 show the comparisons of the self-similar profiles between the model predictions and the measurements for the mixing layer, plane and round jets, respectively. In these figures, the profiles for the mean velocity the Reynolds shear stress and the turbulent kinetic energy are presented. For the mixing layer, the results are shown in a self-similar coordinate η defined as

$$\eta = -\frac{y - y_{0.5}}{y_{0.9} - y_{0.1}}.$$

$y_{0.1}, y_{0.5}$, and $y_{0.9}$ denote the locations where the ratio of the local mean velocity to that of the free stream are 0.1, 0.5, and 0.9, respectively. Figure 2 shows that the mean velocity profiles of the mixing layer predicted by either the present model or the ske model agree well with experimental data of Patel[11]. The present model, however, gives better predictions of the turbulent kinetic energy and the Reynolds shear stress distributions than the ske model. This is especially true for their peak levels. The predictions for the plane jet are shown in Figure 3. The model predictions are compared with the measurements of Gutmark and Wygnanski[12], Bradbury[13], and Hekestad[14]. The predictions given by both the present model and the ske model agree well with the experimental data. The turbulent kinetic energy level at the jet centerline is slightly lower than the measured values. For the round jet, the comparisons are made between the model predictions and the measurements of Wygnanski and Fielder[15] and Rodi[16] and are shown in Figure 4. The profile distribution

of the mean velocity predicted by the current model agree well with the Rodi's data, while the ske model predicts a faster spreading of the round jet into the surroundings and a wider distribution. Significant improvement is also achieved in the prediction of the turbulent kinetic energy profile over the ske model in terms of both the centerline level and the overall distribution. The new modeling of the production of the dissipation rate according to its dynamic significance is believed to contribute to these improvements over the ske model. The calculated spreading rates of these flows are compared with measurements and are shown in Table 2.

Table 2. Comparison of the spreading rates of turbulent free shear flows

Case	measurement	ske model	present model
mixing layer	0.13-0.17	0.152	0.144
plane jet	0.105-0.11	0.109	0.103
round jet	0.085-0.095	0.116	0.105

The present model demonstrates better predictions over the ske model; especially, the spreading rate anomaly of plane and round jets are significantly reduced. This improvement is mainly due to the new dissipation rate equation.

5.3 Channel flow and boundary layer flows

Turbulent channel flow and turbulent boundary layer flows with/without pressure gradients were calculated to test the performance of the present model for wall bounded flows. Since the present model is proposed for turbulent flows away from the wall, the integration was carried out down to $y^+ = 80$ rather than to the wall in the calculations. At $y^+ = 80$, DNS values were used as the boundary conditions for the turbulent channel flows and wall functions were used for the turbulent boundary layer flows.

The results for 2D fully developed turbulent channel flow at $Re_\tau = 395$ are shown in Figure 5. This flow was calculated by Kim[17] using direct numerical simulation. Both the present model and the ske model agree reasonably well with the DNS data. Figure 6 shows the results for the flat plate boundary layers with the Reynolds number up to $Re_\theta = 16000$. Here, comparison is made with the experimental results of Wieghardt[18]. Both the present

model and the ske model give good agreement with the experiments. Overall, the present model gives a slightly better prediction for boundary layer development.

Figures 7 shows the results for the Herring and Norbury flow[19], which is the boundary layer flow under favorable pressure gradient. The present model and the ske model give similar predictions for the velocity profile. The ske model gives better predictions for the skin friction coefficient and the shape factor while the present model gives a better prediction for the boundary layer thickness. The turbulent boundary layer under adverse pressure gradient studied by Bradshaw[20] and the turbulent boundary layer under increasingly adverse pressure gradient studied by Samuel and Joubert[21] were also calculated. The results are shown in Figure 8 and Figure 9, respectively. In both cases, the present model gives better predictions, particularly for the skin friction.

5.4 Backward-facing step flows

The performance of the present model for complicated recirculating flows is demonstrated through calculations for two backward-facing step flows, one (DS-case[22]) with smaller and the other (KKJ-case[23]) with larger step height, both of which have been extensively used to benchmark calculations of separated flows. The calculations were performed with a conservative finite-volume procedure. The convection terms of the governing equations were discretized by a second-order accurate and bounded differencing scheme[24], and all the other terms by the standard central differencing scheme. Sufficiently fine grids, with 201×109 points in the DS-case and 199×91 points in the KKJ-case, were used to establish numerical credibility of the solutions. The computational domain had a length of 50 step heights, one fifth of which was placed upstream of the step. The experimental data were used to specify the inflow conditions and the fully-developed flow conditions were imposed at the outflow boundary. The standard wall function approach[25] was used to bridge the viscous sublayer near the wall. The comparison of the predicted and the measured reattachment length is shown in Table 3. Figures 10-14 show the comparsion of the skin friction and pressure distributions along the bottom wall, and the mean velocity as well as the turbulent stress profiles at three downstream locations. All the quantities were normalized by the step height h and the experimental reference free-stream velocity U_{ref}.

Table 3. Comparison of the reattachment point locations

Case	measurement	ske model	present model
DS	6.1	4.99	5.36
KKJ	7± 0.5	6.35	6.8

It can be seen that the overall performance of the present model is better than that of the ske model.

6. Concluding Remarks

A new dissipation rate equation based on an analysis of the dynamic equation for fluctuating vorticity is proposed. The form of the model equation is consistent with the one based on the spectral energy cascade model introduced by Lumley[6]. The proposed dissipation rate equation can be readily applied to any level of turbulence closures. In the present study, it has been applied to the new eddy viscosity model described in Section 4.1 and tested in various benchmark flows including: rotating homogeneous shear flows; boundary-free shear flows; channel and flat boundary layer flows with and without pressure gradients; and backward facing step flows. The results show that the present model performs better than the standard $k-\varepsilon$ model in almost all of the cases tested. The new model dissipation rate equation is expected to enhance the numerical stability of turbulence model equations, especially when it is used in conjunction with the advanced closure schemes, such as second order closures. We have just finished implementing the present model into the LRR[26] second order closure. Preliminary results seem to show that the initial decay behavior of and the effect of rotation on both k and ε of initially isotropic rotating homogeneous shear flows are well captured.

References

[1] Jones, W. P. and Launder, B. E., "The calculation of low-Reynolds number phenomena with a two-equation model of turbulence," *International Journal of Heat and Mass Transfer*, Vol. 16, 1973, pp. 1119-1130.

[2] Chien, K. Y., "Predictions of Channel and boundary layer flow with a low-Reynolds-

number turbulence model," *AIAA Journal*, Vol. 20, 1982, pp. 33-38.

[3] Yang, Z. and Shih, T.-H., "A new time scale based $k-\varepsilon$ model for near wall turbulence," NASA TM 105768, 1992.

[4] Shih, T.-H. and Lumley, J. L.,"Kolmogorov behavior of near-wall turbulence and its application in turbulence modeling," NASA TM 105663.

[5] Bardina, J., Ferziger, J. H., and Reynolds, W. C., "Improved turbulence models based on large eddy simulation of homogeneous, incompressible, turbulent flows," Rept. No. TF-19, Stanford University, Stanford, CA., 1983.

[6] Lumley, J. L,"Some comments on turbulence," *Phys. Fluids*, Vol. 4, 1992, pp.203-211.

[7] Tennekes, H. and Lumley, J. L., *A First Course in Turbulence*, The MIT press (1972).

[8] M.S. Mohamed and J.C. Larue, "The decay power law in grid-generated turbulence," *Journal of Fluid Mechanics*, Vol. 219, 1990, pp.195-214.

[9] Tovalarison, S. and Corrsin, S., "Experiments in nearly homegeneous turbulent shear flow with a uniform mean temperature gradient," *Journal of Fluid Mechanics*, Vol. 104, 1981, pp.311-347.

[10] Shih, T.-H., Zhu, J., and Lumley, J. L. , "A realizable Reynolds stress algebraic equation model," NASA TM 105993, 1992.

[11] Patel, R. P., "An experimental study of a plane mixing layer," *AIAA Journal*, Vol. 29, 1973, pp.67-71.

[12] Gutmark, E. and Wygnanski, I., "The planner turbulent jet," *Journal of Fluid Mechanics*, Vol. 73, 1976, pp.465-495,

[13] Bradbury, L. J. S., "The structure of the self-preserving jet," *Journal of Fluid Mechanics*, Vol. 23, 1965, pp.31-64.

[14] Hekestad, G., "Hot-wire measurements in a plane turbulent jet," *Journal of Fluid*

Mechanics, Vol. 32, 1965, pp.721-734.

[15] Wygnanski, I. and Fiedler, H. E., "The two-dimensional mixing region," *Journal of Fluid Mechanics*, Vol. 41, 1970, pp.327-361.

[16] Rodi, W., "A new method of analyzing hot-wire signals in highly turbulent flow and its evaluation in round jets," Disa Information 1975, No. 17.

[17] Kim, J., private communication.

[18] Wieghardt, K., "Equilibrium boundary layer at constant pressure," *Computation of Turbulent Boundary Layers-1968 AFSOR-IFP-Stanford University*, Coles, D. E. and Hirst, E. A. edt., Vol. 2, pp.98-123.

[19] Herring, H. and Norbury, J., "Equilibrium boundary layer in mild negative pressure gradient," *Computation of Turbulent Boundary Layers-1968 AFSOR-IFP-Stanford University*, Coles, D. E. and Hirst, E. A. edt., Vol.2, pp.249-258.

[20] Bradshaw, P., "Equilibrium boundary layer in moderate positive pressure gradient," *Computation of Turbulent Boundary Layers-1968 AFSOR-IFP-Stanford University*, Coles, D. E. and Hirst, E. A. edt., Vol.2, pp.241-248.

[21] Samuel, A.E., and Joubert, P.N., "A boundary Layer Developing in an Increasingly Adverse Pressure Gradient," *Journal of Fluid Mechanics*, Vol. 66, 1974, pp.481-505.

[22] Driver, D. M. and Seegmiller, H. L., "Features of a reattaching turbulent shear layer in divergent channel flow", *AIAA Journal*, Vol.23, 1985, pp.163-171.

[23] Kim, J., Kline, S. J. and Johnston, J. P., "Investigation of separation and reattachment of a turbulent shear layer: Flow over a backward-facing step", Rept. MD-37, Thermosciences Div., Dept. of Mech. Eng., Stanford University, 1978.

[24] Zhu, J., "A low diffusive and oscillation-free convection scheme", *Comm. App. Num. Methods.*, Vol.7, 1991, pp.225-232.

[25] Launder, B. E. and Spalding, D. B., "The numerical computation of turbulent flows",

Comput. Meths. App. Mech. Eng., Vol.3, 1974, pp.269-289.

[26] Launder, B. E., Reece, G. J., and Rodi, W., "Progress in the Development of a Reynolds-stress Turbulence Closure," *Journal of Fluid Mechanics*, Vol 68, 1974, pp. 537-566.

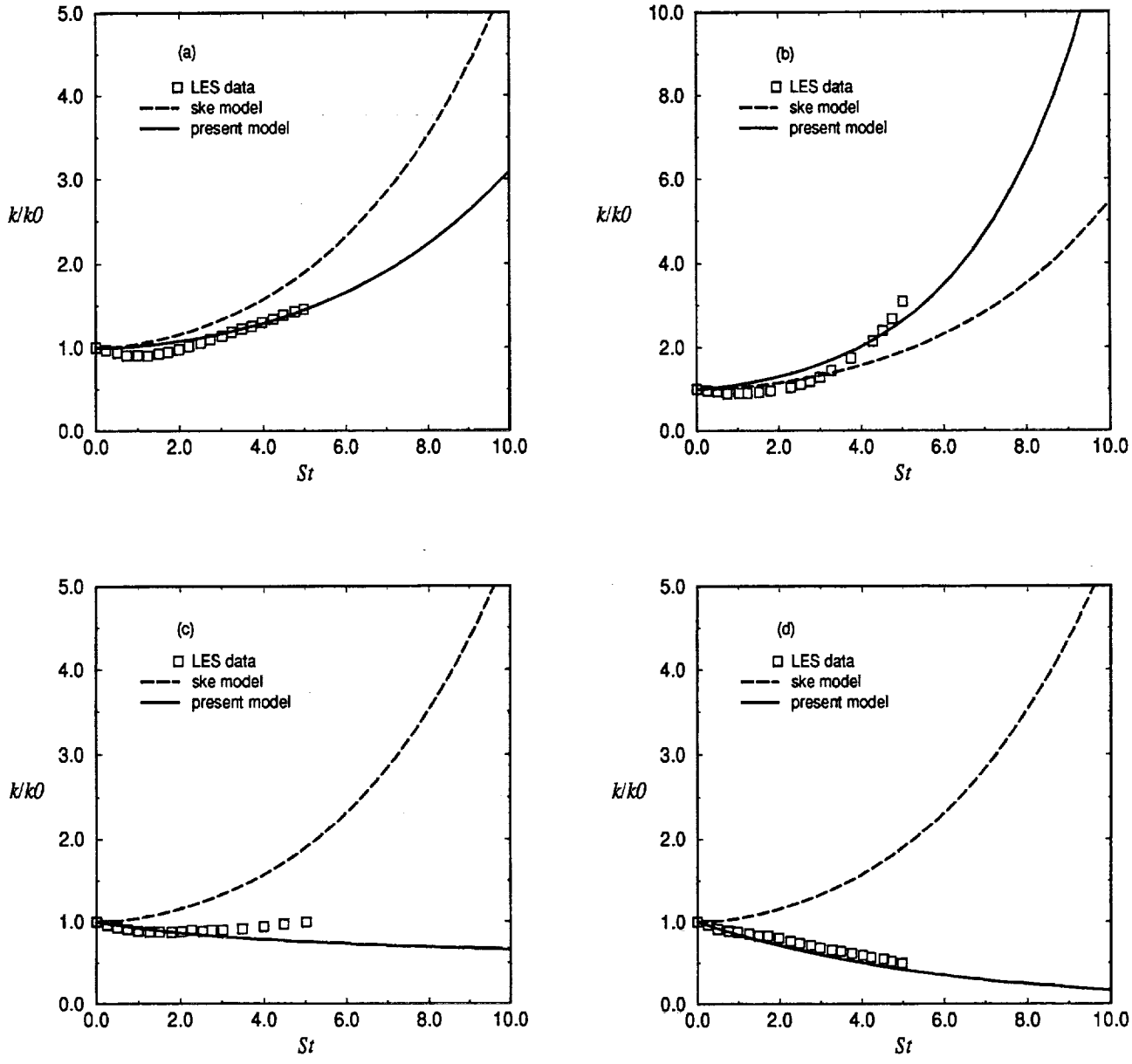

Figure 1. Rotating homogeneous shear flows. (a) Ω/S=0.0; (b) Ω/S=0.25; (c) Ω/S=0.5; (d) Ω/S=-0.5.

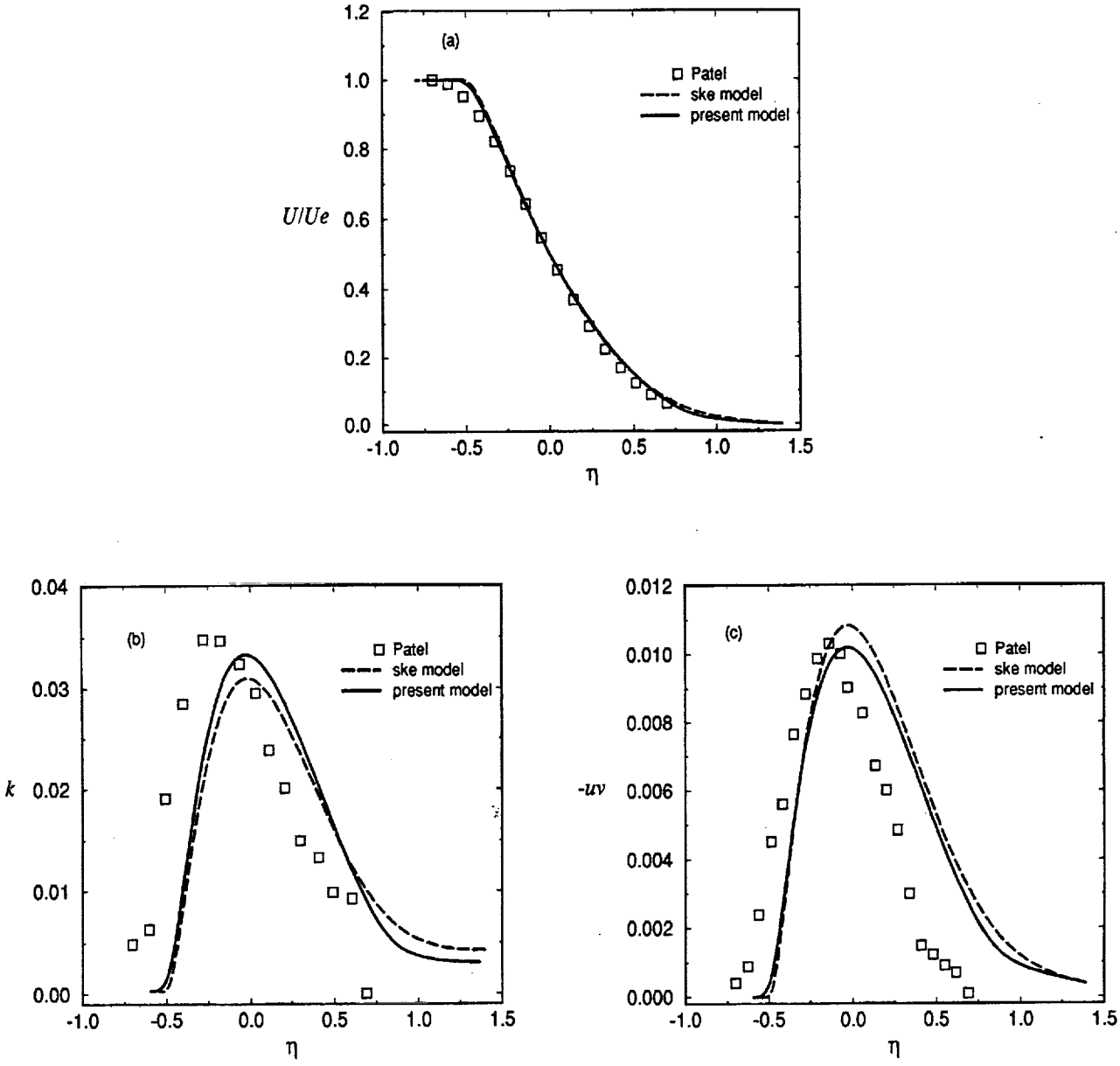

Figure 2. Self-similar profiles for a plane mixing layer. (a) mean velocity; (b) turbulent kinetic energy; (c) Reynolds shear stress.

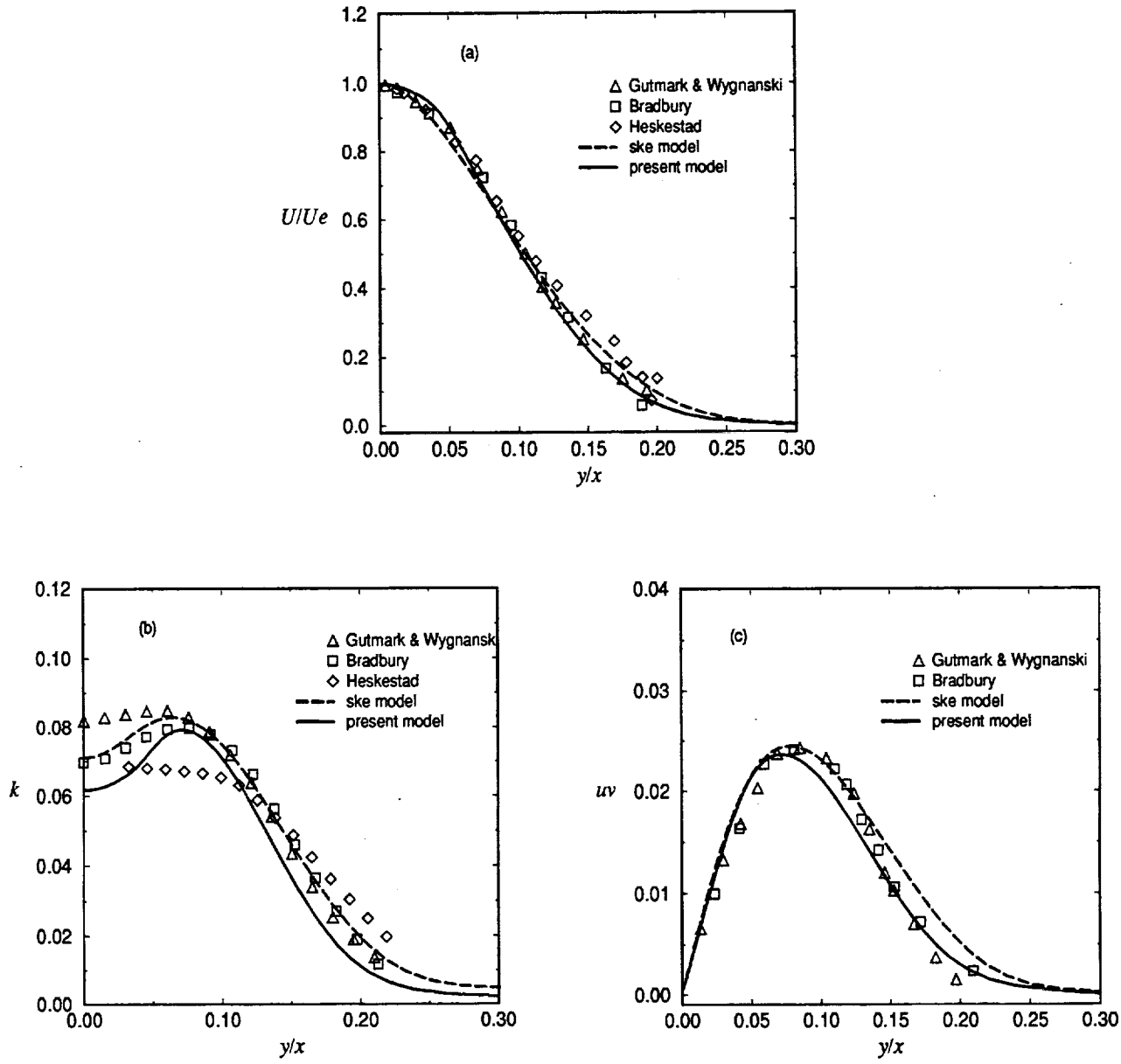

Figure 3. Self-similar profiles for a plane jet. (a) mean velocity; (b) turbulent kinetic energy; (c) Reynolds shear stress.

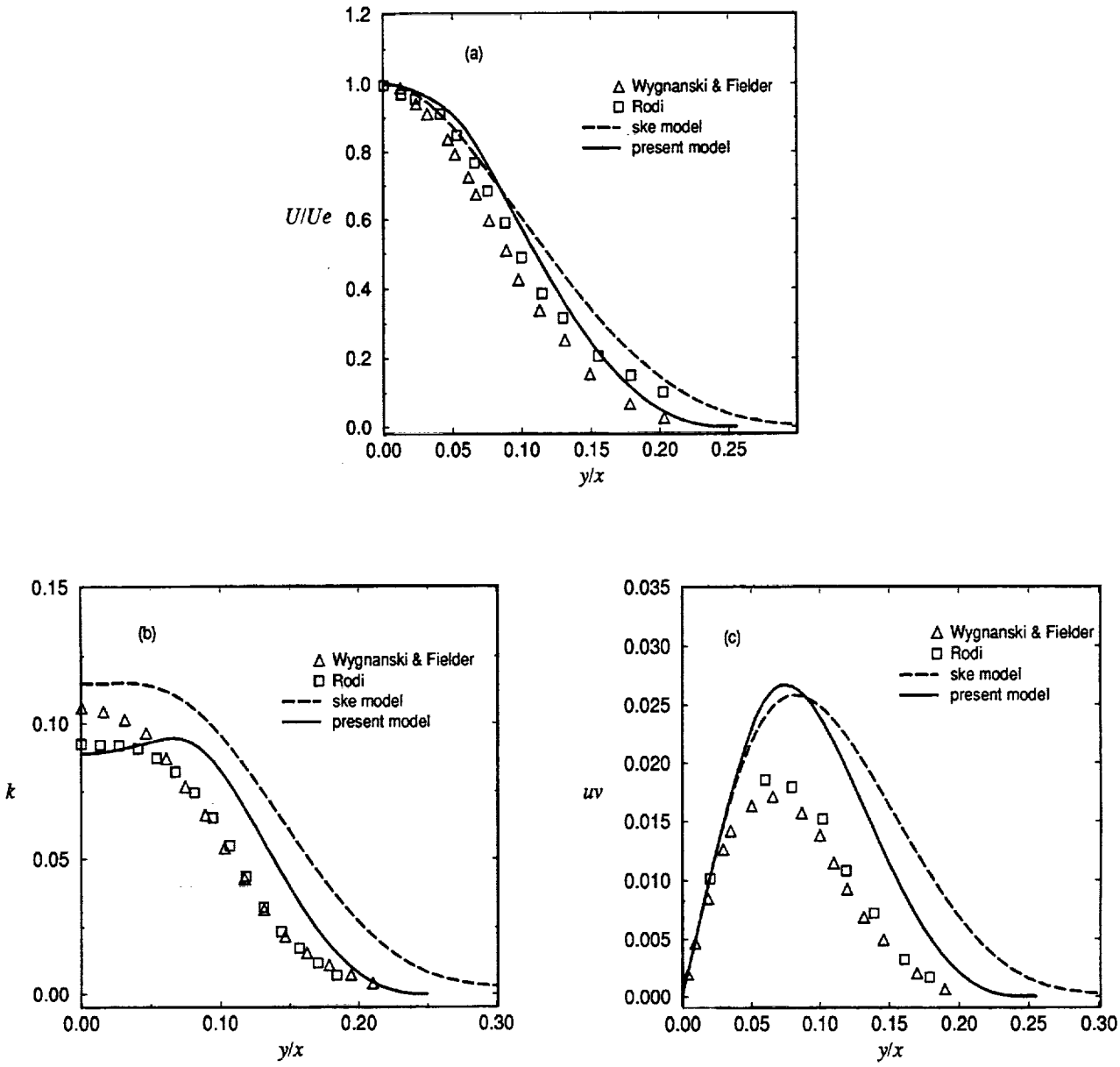

Figure 4. Self-similar profiles for a round jet. (a) mean velocity; (b) turbulent kinetic energy; (c) Reynolds shear stress.

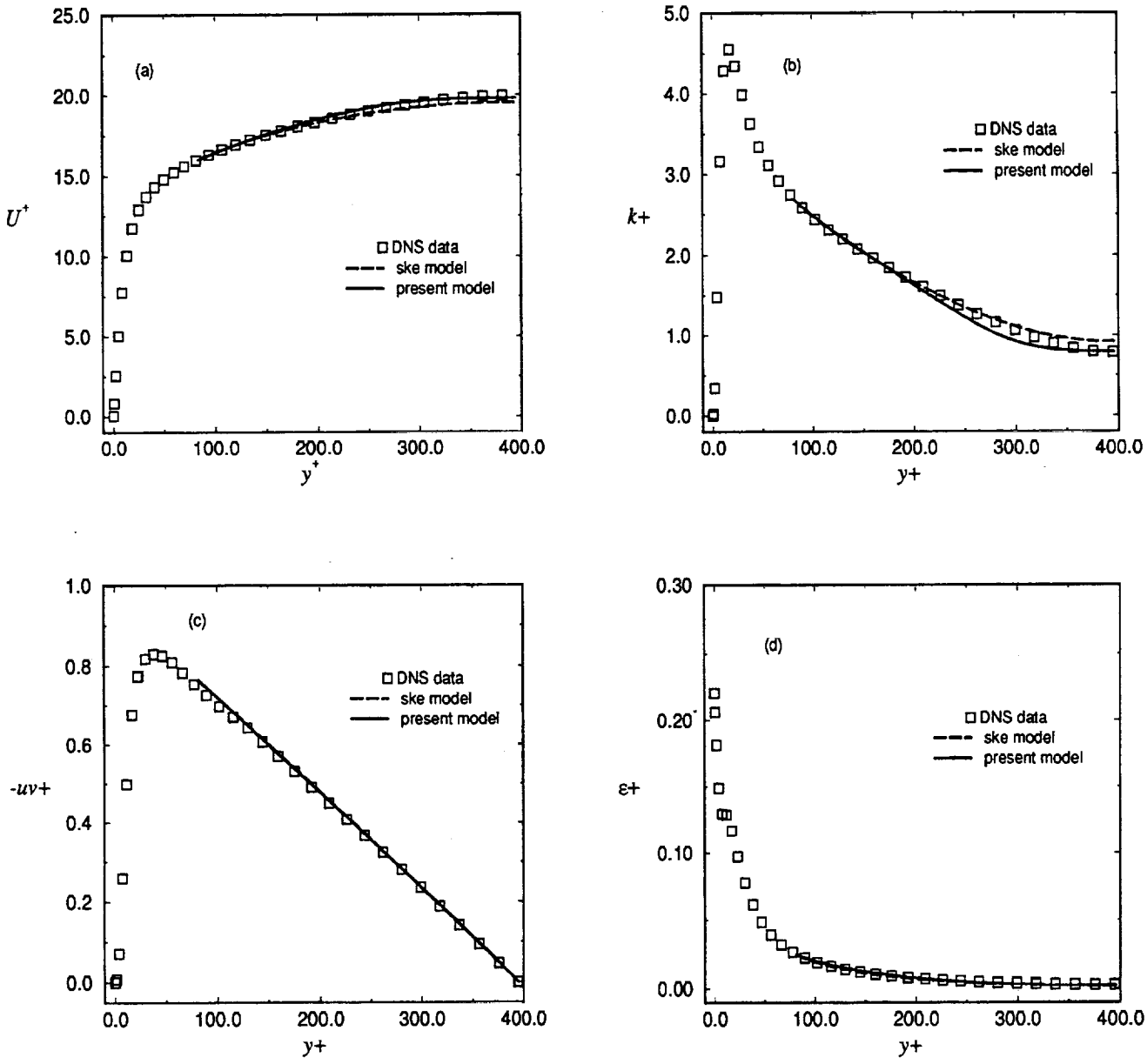

Figure 5. Turbulent channel flow at $Re_\tau = 395$. (a) mean velocity; (b) turbulent kinetic energy; (c) turbulent shear stress; (d) dissipation rate.

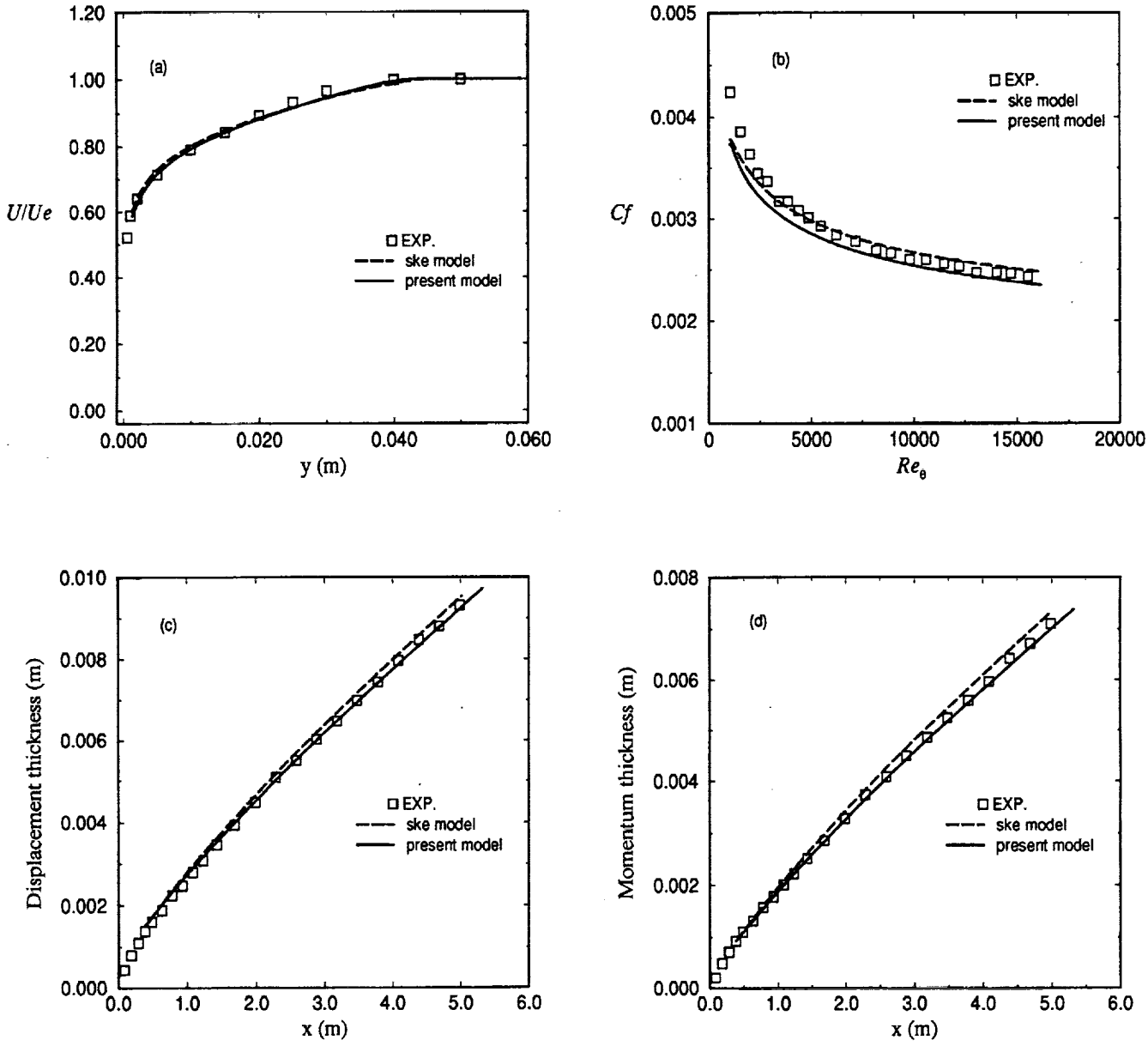

Figure 6. Zero pressure gradient turbulent boundary layer. (a) mean velocity at Re_θ=8900; (b) skin friction coefficient; (d) displacement thickness; (d) momentum thickness.

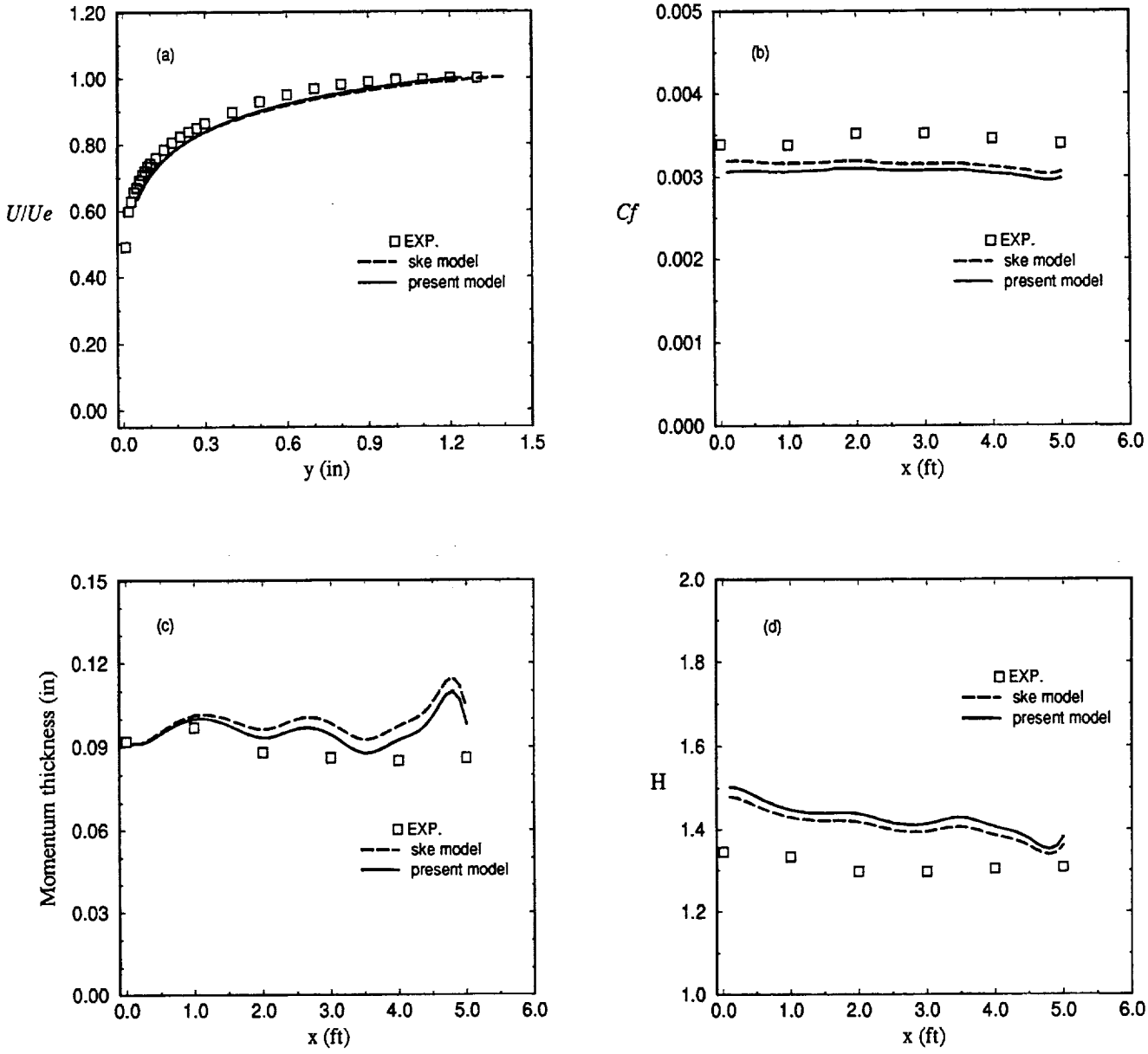

Figure 7. Favorable pressure gradient turbulent boundary layer (Herring and Norbury flow). (a) mean velocity at x=4.0 ft.; (b) skin friction coefficient; (c) momentum thickness; (d) shape factor.

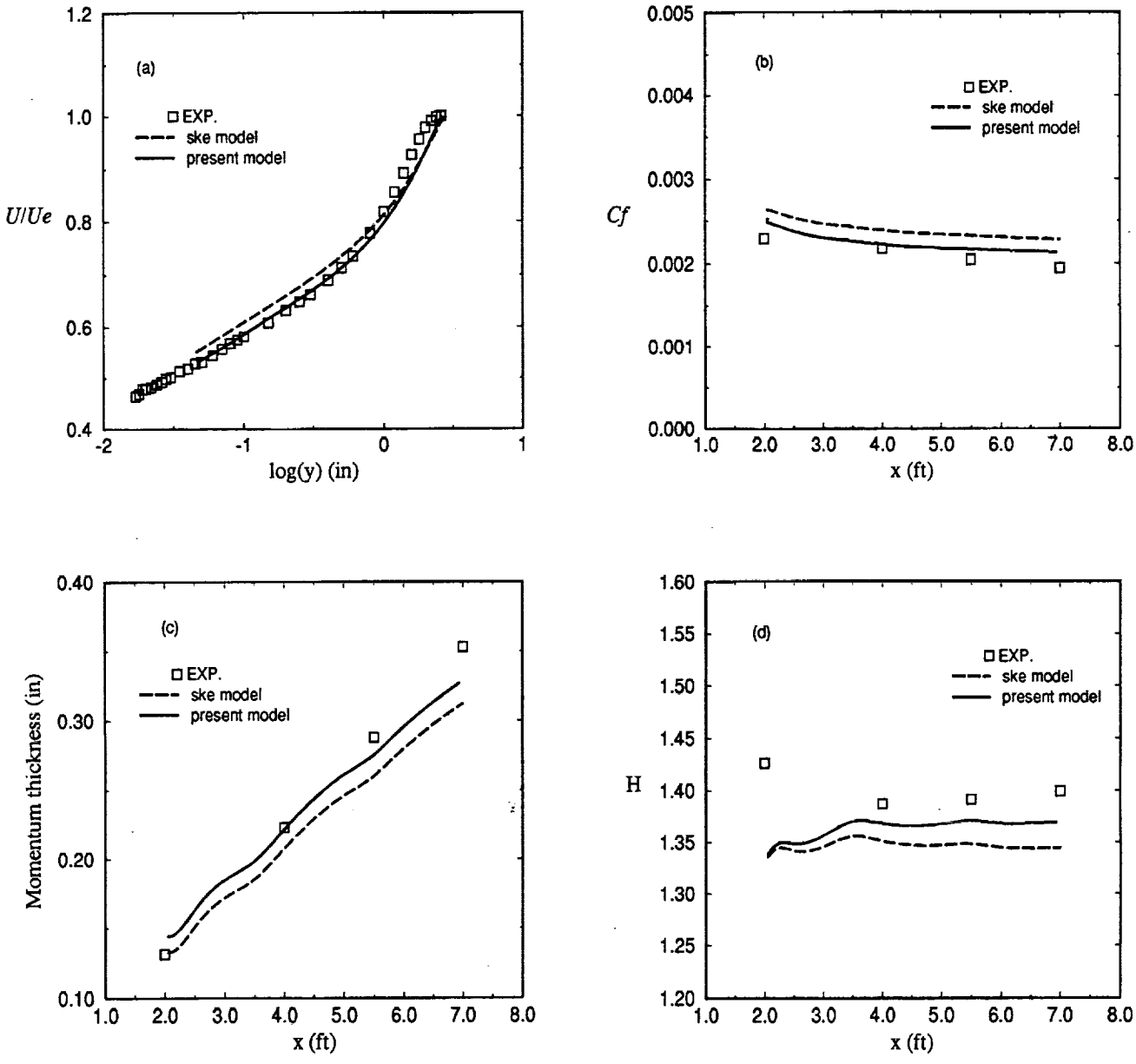

Figure 8. Adverse pressure gradient turbulent boundary layer (Bradshaw flow). (a) mean velocity at x=5.5 ft.; (b) skin friction coefficient; (c) momentum thickness; (d) shape factor.

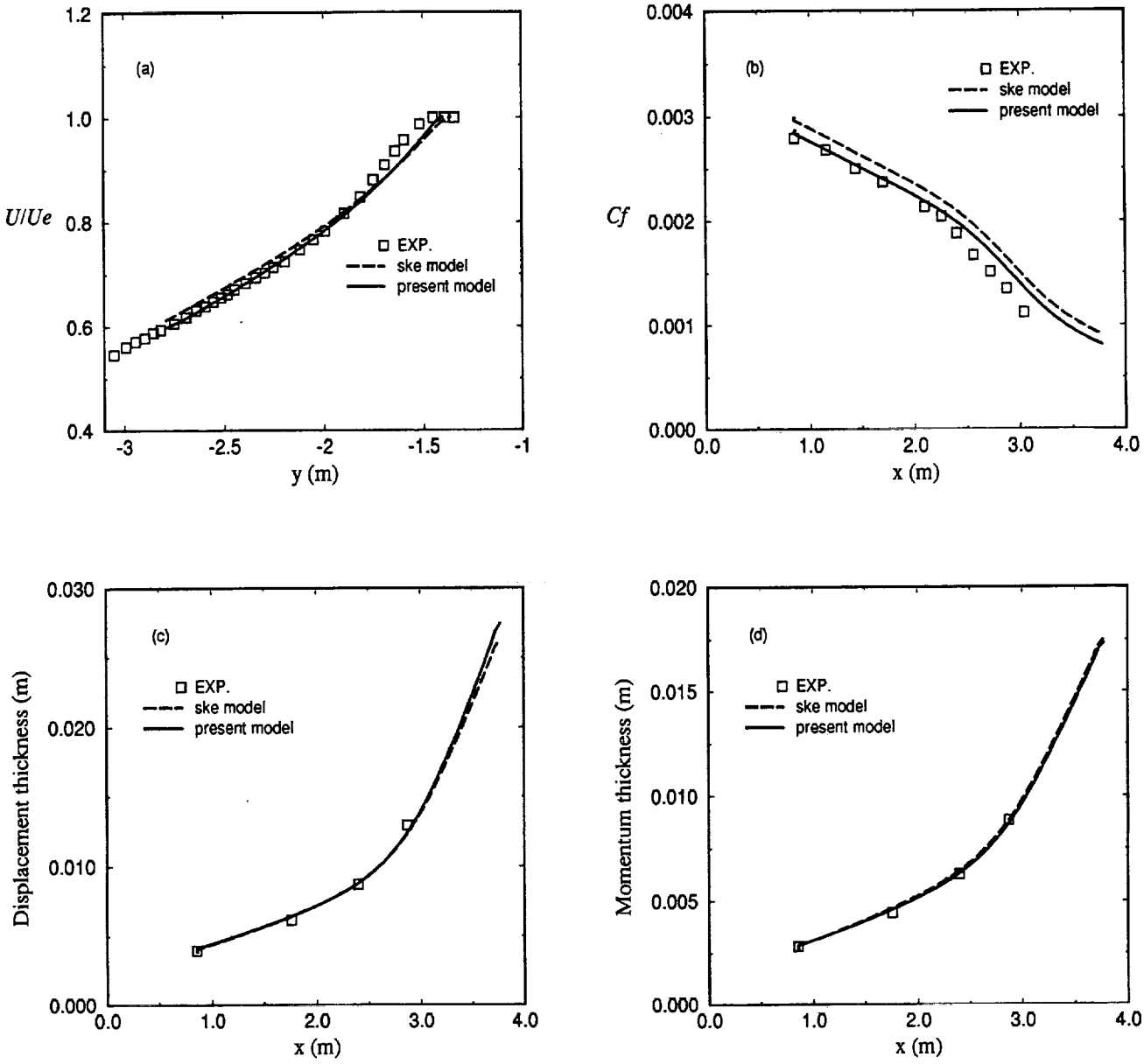

Figure 9. Adverse pressure gradient turbulent boundary layer (Samuel and Joubert flow). (a) mean velocity at x=1.76 m.; (b) skin friction coefficient; (c) displacement thickness; (d) momentum thickness.

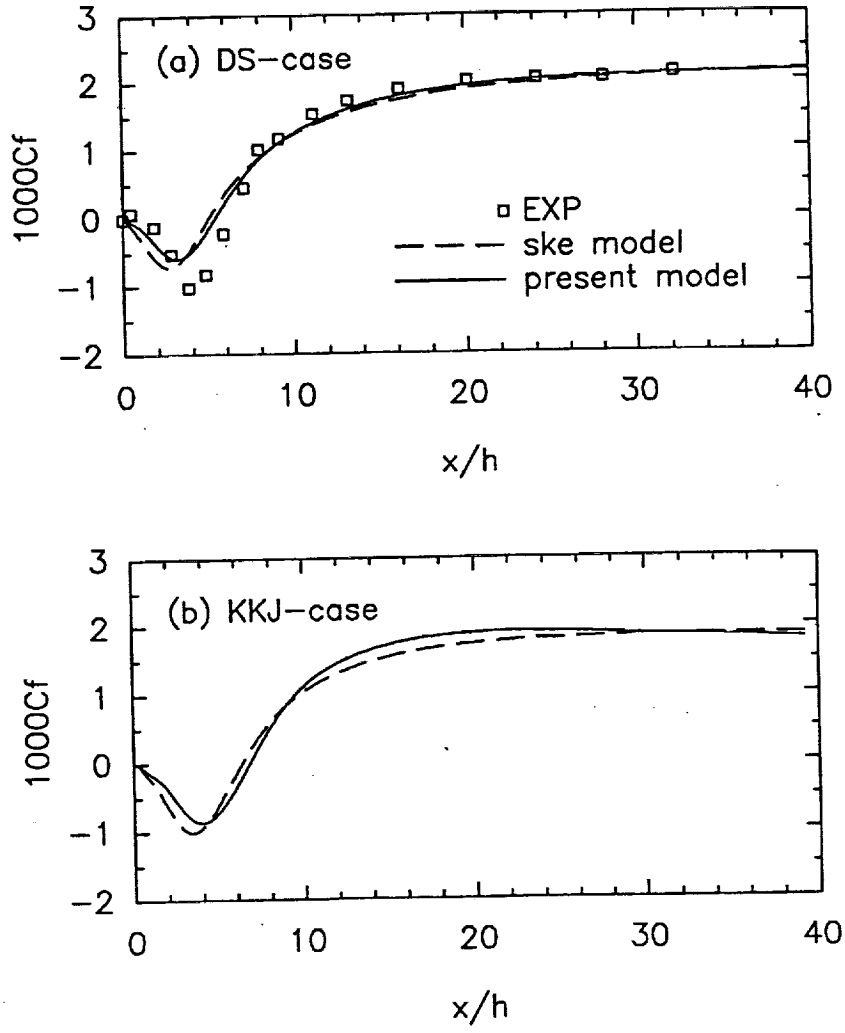

Figure 10. Friction coefficient C_f along the bottom wall

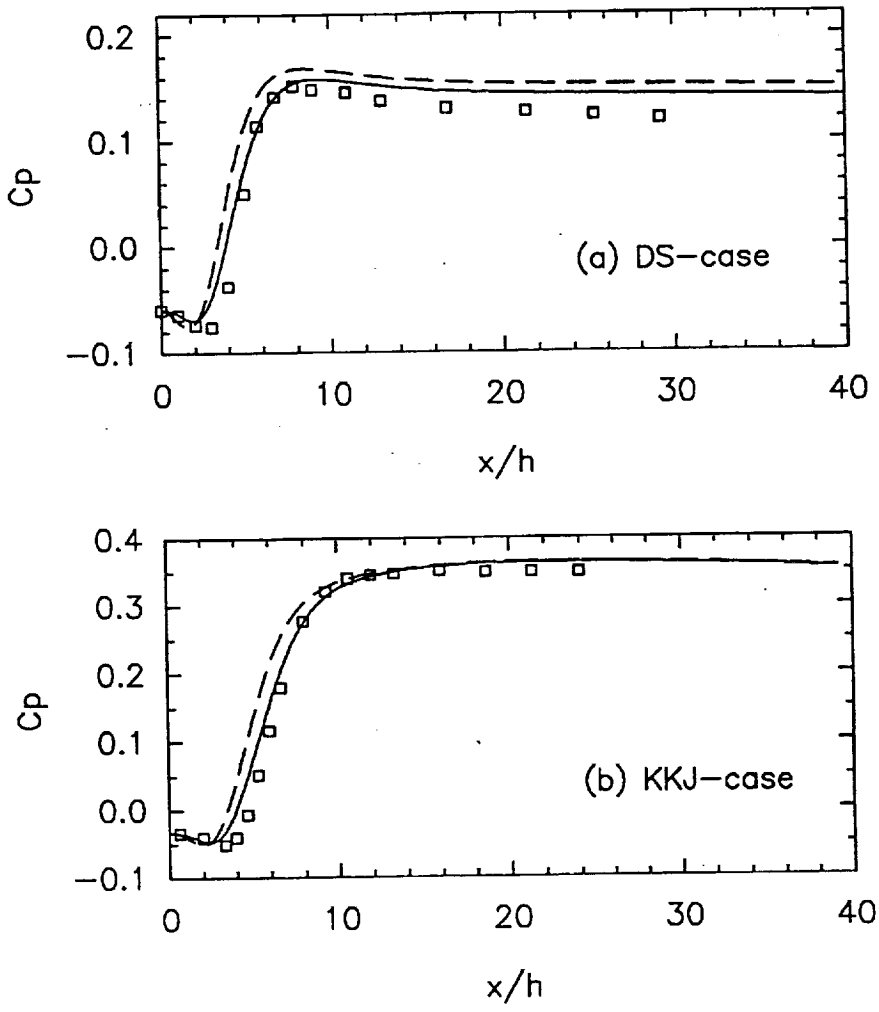

Figure 11. Static pressure coefficient C_p along the bottom wall (legend as in figure 10)

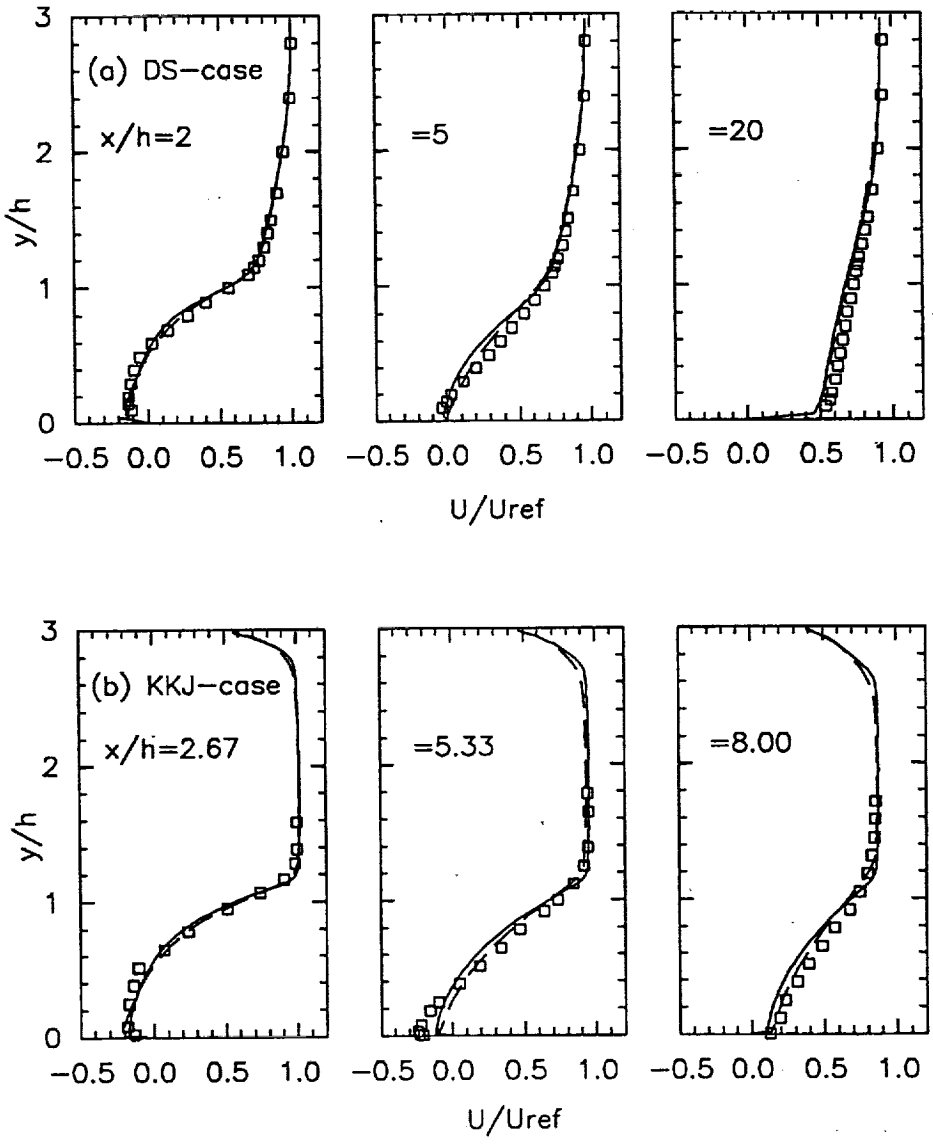

Figure 12. Streamwise mean velocity U-profiles
(legend as in figure 10)

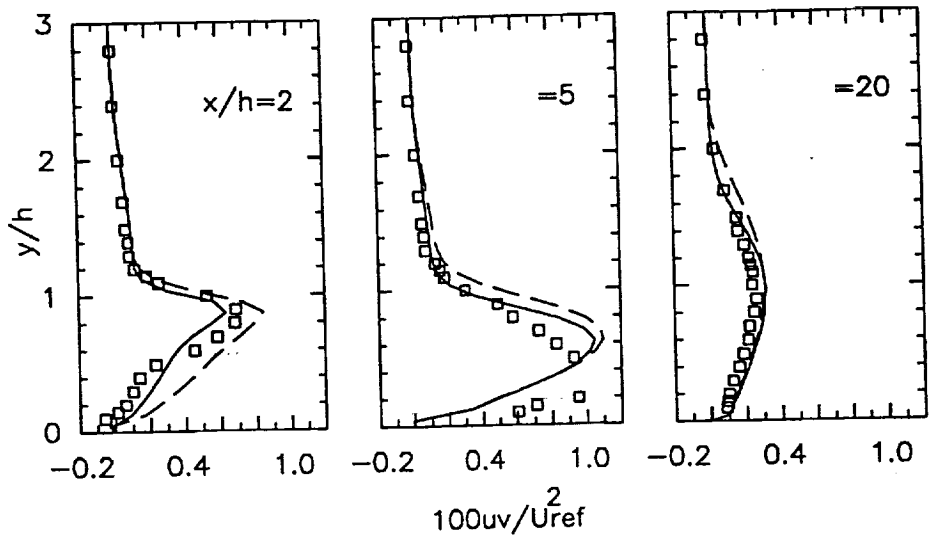

Figure 13. Turbulent shear stress profiles in the DS-case
(legend as in figure 10)

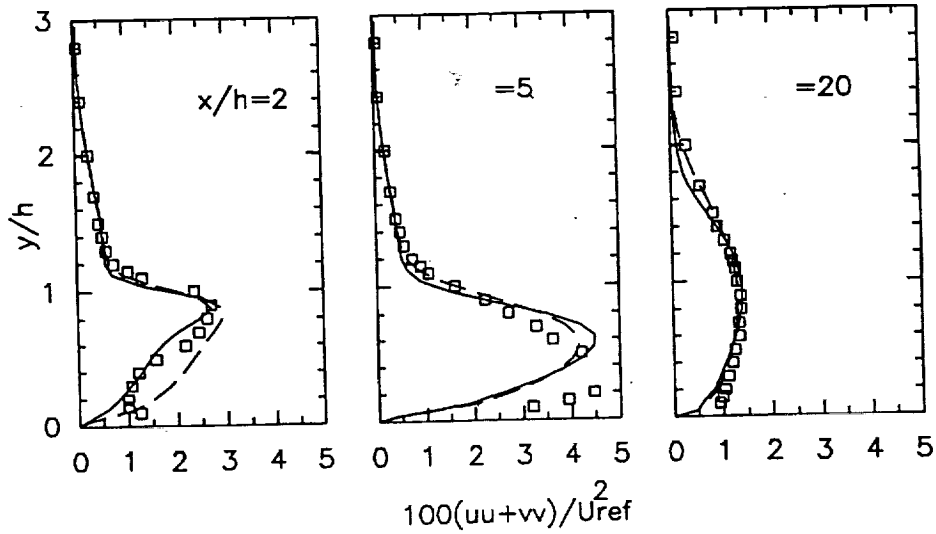

Figure 14. Turbulent normal stress profiles in the DS-case
(legend as in figure 10)

REPORT DOCUMENTATION PAGE

Form Approved
OMB No. 0704-0188

1. AGENCY USE ONLY (*Leave blank*)	2. REPORT DATE	3. REPORT TYPE AND DATES COVERED
	January 1994	Technical Memorandum

4. TITLE AND SUBTITLE

A Vorticity Dynamics Based Model for the Turbulent Dissipation—Model Development and Validation

5. FUNDING NUMBERS

WU-505-90-5K

6. AUTHOR(S)

Tsan-Hsing Shih, William W. Liou, Aamir Shabbir, Zhigang Yang, and Jiang Zhu

7. PERFORMING ORGANIZATION NAME(S) AND ADDRESS(ES)

National Aeronautics and Space Administration
Lewis Research Center
Cleveland, Ohio 44135-3191

8. PERFORMING ORGANIZATION REPORT NUMBER

E-7877

9. SPONSORING/MONITORING AGENCY NAME(S) AND ADDRESS(ES)

National Aeronautics and Space Administration
Washington, D.C. 20546-0001

10. SPONSORING/MONITORING AGENCY REPORT NUMBER

NASA TM-106177
ICOMP-93-20
CMOTT-93-08

11. SUPPLEMENTARY NOTES

Tsan-Hsing Shih, William W. Liou, Aamir Shabbir, Zhigang Yang, and Jiang Zhu, Institute for Computational Mechanics in Propulsion and Center for Modeling of Turbulence and Transition, NASA Lewis Research Center, (work funded under NASA Cooperative Agreement NCC3-233). ICOMP Program Director, Louis A. Povinelli, (216) 433-5818.

12a. DISTRIBUTION/AVAILABILITY STATEMENT

Unclassified - Unlimited
Subject Category 34

12b. DISTRIBUTION CODE

13. ABSTRACT (*Maximum 200 words*)

A new model dissipation rate equation is proposed based on the dynamic equation of the mean-square vorticity fluctuation for large Reynolds number turbulence. The advantage of working with the vorticity fluctuation equation is that the physical meanings of the terms in this equation are more clear than those in the dissipation rate equation. Hence, the model development based on the vorticity fluctuation equation is more straightforward. The resulting form of the model equation is consistent with the spectral energy cascade analysis introduced by Lumley (1992). The proposed model dissipation rate equation is numerically well behaved and can be applied to any level of turbulence modeling. In the present study, it is applied to a realizable eddy viscosity model. Flows that are examined include: (i) rotating homogeneous shear flows; (ii) free shear flows; (iii) a channel flow and flat plate boundary layers with and without pressure gradients; and (iv) backward facing step separated flows. In most cases, the present model predictions show considerable improvement over the standard κ-ε model.

14. SUBJECT TERMS

Turbulence modeling

15. NUMBER OF PAGES

31

16. PRICE CODE

A03

17. SECURITY CLASSIFICATION OF REPORT	18. SECURITY CLASSIFICATION OF THIS PAGE	19. SECURITY CLASSIFICATION OF ABSTRACT	20. LIMITATION OF ABSTRACT
Unclassified	Unclassified	Unclassified	